Paper 17

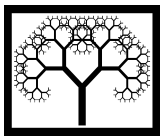

Proceedings of the Twelfth International Conference
on Computational Structures Technology,
B.H.V. Topping and P. Iványi, (Editors),
Civil-Comp Press, Stirlingshire, Scotland.

Transient Response of Delaminated Torsion Stiff Composite Conical Shell Panels subjected to a Low Velocity Oblique Impact

S. Dey, T. Mukhopadhyay and S. Adhikari
College of Engineering
Swansea University, United Kingdom

Abstract

This paper investigates the low velocity oblique impact responses of delaminated torsion stiff composite pretwisted shallow conical shells. An eight-node isoparametric quadratic plate bending element is employed in the finite element formulation incorporating rotary inertia and the effects of transverse shear deformation based on Mindlin's theory. The modified Hertzian contact law is employed to evaluate the impact parameters, and the time-dependent equations are solved using Newmark's time integration scheme. Parametric studies are carried out to investigate the effects of triggering parameters such as twist angle, and the oblique angle when subjected to low velocity impact by a solid sphere at the centre.

Keywords: oblique impact, delamination, torsion stiff, finite element, contact force.

1 Introduction

The impact on aircraft and spacecraft structures is common phenomenon in aerospace industry such as bird-strike, runway debris collision and similar loading events. In real life situation, such impact may cause in the interior of the composite materials, which will grow progressively and result in catastrophic failure of the structure. It is therefore, important to investigate the effect of impact motivated by practical situations encountered in the aerospace, marine, automotive and other industries wherein the composite materials are extensively employed. Composite materials are extensively used not only due to their high strength and stiffness but also for the provision of tailoring of material properties and cost effectiveness in weight sensitive applications. Among the wide spectrum of advantages, the threat of composites is low through the thickness strength due to weakness in transverse shear deformation. The pioneering investigation on twisted composite plates was conducted by Qatu and Leissa [1] to obtain natural frequencies of stationary plates using Ritz method. Sun and Chen [2] studied the impact response of initially

stressed laminate using two dimensional finite element analyses and reported the effects of impactor velocity, impactor mass and the initial stress on the impact response of the laminate. Karmakar and Kishimoto [3] undertook a transient dynamic finite element analysis to investigate the response characteristics of centrally impacted delaminated composite pretwisted rotating cylindrical shells due to low velocity impact. The failure analysis of composite plate due to bending and impact was numerically investigated by Parhi et al. [4] using finite element method.

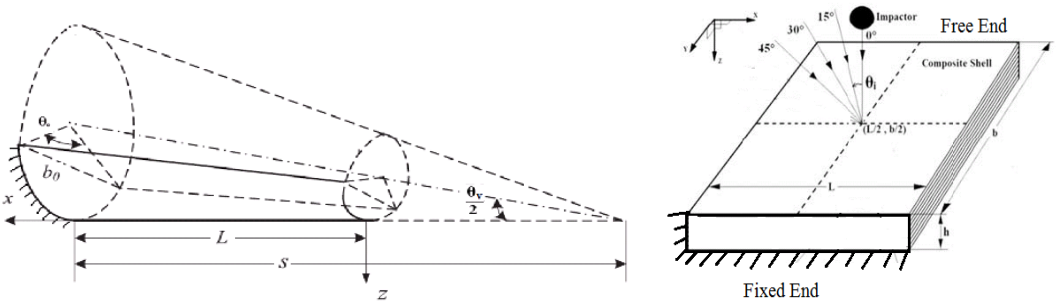

(a) (b)

Figure 1: Geometry of conical shell panel

Nomenclature

R_x , R_y	radius of curvature in x-direction and y-direction, respectively
R_{xy}	radius of twist
Ψ, ζ	twist angle and oblique impact angle
ρ, υ	mass density and Poisson's ratio, respectively
L, bo	length and reference width, respectively
h, a	thickness and crack length, respectively
d	distance of centreline of delamination from fixed end
θ_v , θ_o	vertex angle and base subtended angle of cone, respectively
[M]	global mass matrix
[K]	elastic stiffness matrix
$[K_\sigma]$	geometric stiffness matrix
{P}	force vector
{δ}	global displacement matrix
C_f	contact force
M_i , $\ddot{\omega}_i$	mass and acceleration of impactor, respectively
Δt	time step
L/s	aspect ratio
n	number of ply
VOI	initial velocity of impactor

Pretwisted composite shallow conical shell could be idealized as turbomachinery blade. The present work is aimed at investigating the effects of delamination on low velocity oblique impact response of torsion stiff composite pretwisted composite shallow conical shells. Torsion stiff [(45°/-45°/-45°/45°)s] configuration represents the laminate which is attributes to high stiffness in torsional mode. To satisfy the compatibility of deformation and equilibrium of resultant forces and moments at the delamination crack front, a multipoint constraint algorithm [5] is incorporated. The modified Hertzian contact law which accounts for permanent indentation is utilized to compute the contact force, and the time dependent equations are solved by Newmark's integration scheme [6].

2 Governing Equations

The governing equations are derived based on Mindlin's Theory incorporating rotary inertia, transverse shear deformation and modified Hertzian contact law. A shallow shell is characterized by its middle surface and is defined by equation [7],

$$z = -\frac{1}{2}\left[\frac{x^2}{R_x} + 2\,\frac{xy}{R_{xy}} + \frac{y^2}{R_y}\right] \tag{1}$$

The radius of twist (R_{xy}), length (L) of shell and twist angle (Ψ) are related as,

$$\tan\psi = -\frac{L}{R_{xy}} \tag{2}$$

The dynamic equilibrium equation for moderate rotational speeds neglecting Coriolis effect is derived employing Lagrange's equation of motion and equation in global form expressed as [8],

$$[M]\{\ddot{\delta}\} + ([K] + [K_\sigma])\{\delta\} = \{P\} \tag{3}$$

where {P} is force vector and {δ} is global displacement vector. $[K_\sigma]$ depends on initial stress distribution and is obtained by iterative procedure upon solving [9],

$$([K] + [K_\sigma])\ \{\delta\} = \{P(\Omega^2)\} \tag{4}$$

For the impact problem, {P} is given as

$$\{P\} = \{0\ 0\ 0 \ldots\ldots .. C_f \ldots\ldots .. 0\ 0\ 0\}^T \tag{5}$$

where C_f is the contact force and the equation of motion of the rigid impactor is obtained as [2],

$$M_i\,\ddot{\omega}_i + C_f = 0 \tag{6}$$

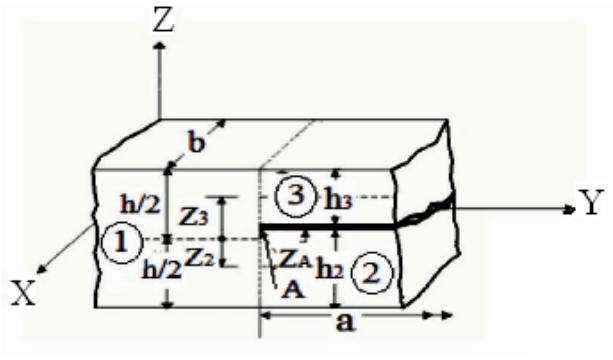

Figure 2: Plate elements at a delamination crack tip [5]

2.1 Multipoint constraint

The sectional view of a typical debonded crack tip is furnished in Figure 2. The nodal displacements of elements 2 and 3 at crack tip expressed [5]

$$U_j = U'_j - (z - z'_j)\,\theta_{xj}\,, \quad V_j = V'_j - (z - z'_j)\,\theta_{yj}\,, \quad W_j = W'_j \text{ (where, } j = 2, 3) \qquad (7)$$

where z'_j is the z-coordinate of mid-plane of element j and the above equation also holds good for element 1 and z'_1 equal to zero. The transverse displacements and rotations at a common node have values expressed as,

$$W_1 = W_2 = W_3 = W, \quad \theta_{x1} = \theta_{x2} = \theta_{x3} = \theta_x\,, \quad \theta_{y1} = \theta_{y2} = \theta_{y3} = \theta_y \qquad (8)$$

In-plane displacements of all three elements at crack tip are equal and they are related as

$$U'_2 = U'_1 - z'_2\,\theta_x\,, \quad V'_2 = V'_1 - z'_2\,\theta_y\,, \quad U'_3 = U'_1 - z'_3\,\theta_x\,, \quad V'_3 = V'_1 - z'_3\,\theta_y \qquad (9)$$

where u'_1 is the mid-plane displacement of element 1. Equations of (8) and (9) relating the nodal displacements and rotations of elements 1, 2 and 3 at the debonded crack tip, are the multipoint constraint equations used in finite element formulation to satisfy the compatibility of displacements and rotations. Mid-plane strains between elements 2 and 3 are related as,

$$\{\varepsilon'\}_j = \{\varepsilon'\}_1 + z'_j\,\{kc_1\} \qquad (10)$$

where $\{\varepsilon'\}$ and $\{kc_1\}$ are the strain vector and the curvature vector, respectively. This equation can be considered as a special case for element 1 and z'_1 is equal to zero. In-plane stress-resultants, {N} and moment resultants, {M} of elements 2 and 3 can be expressed as,

$$\{N\}_j = [A]_j\,\{\varepsilon'\}_1 + (z'_j\,[A]_j + [B]_j)\,\{kc_1\} \quad (\text{where } j = 2, 3) \qquad (11)$$

$$\{M\}_j = [B]_j\,\{\varepsilon'\}_1 + (z'_j\,[B]_j + [D]_j)\,\{kc_1\} \quad (\text{where } j = 2, 3) \qquad (12)$$

where [A], [B] and [D] are the extension, bending-extension coupling and bending stiffness coefficients of the composite laminate, respectively.

2.2 Contact force

The contact force is assumed to be a point load and impact surface of the impactor is considered to be spherical. During loading, contact force can be evaluated as [2]

$$C_f = k\,\alpha^{1.5}, \qquad 0 < \alpha \le \alpha_m \tag{13}$$

where k is the contact stiffness and α is the local indentation i.e., change in distance between centre of the impactor and the mid-surface of target shell. The modified contact stiffness of the Hertzian contact theory [10] proposed as,

$$k = \frac{4}{3}\sqrt{R_i}\,\frac{1}{[(1-\upsilon_i^2)/E_i \;+\; 1/E_{yy}]} \tag{14}$$

where R_i, υ_i and E_i are the radius, Poisson's ratio and Young's modulus of elasticity of the impactor, respectively and E_{yy} is the modulus of elasticity of the uppermost composite ply in the direction transverse to the fibres. Upon unloading and loading, the contact forces are simulated by the following relation

$$C_f = C_m\,[\frac{\alpha-\alpha_o}{\alpha_m-\alpha_o}]^{5/2} \quad and \quad C_f = C_m\,[\frac{\alpha-\alpha_o}{\alpha_m-\alpha_o}]^{3/2} \tag{15}$$

where C_m is the maximum contact force at the beginning of unloading and α_m is the maximum indentation during loading. The permanent indentation (α_o) in a loading-unloading cycle is determined as

$$\begin{aligned} &\alpha_o = 0 && \text{when } \alpha_m < \alpha_{cr}, \text{ and} \\ &\alpha_o = \beta_c(\alpha_m - \alpha_{cr}) && \text{when } \alpha_m \ge \alpha_{cr} \end{aligned} \tag{16}$$

where β_c is a constant and α_{cr} is the critical indentation beyond which permanent indentation occurs, and the respective values are 0.094 and 1.667×10^{-2} cm for graphite-epoxy composite. For impact the local indentation is formulated as [11],

$$\alpha(t) = w_i(t)\,\mathrm{Cos}\,\zeta_i - w_p(x_c, y_c, t)\,\mathrm{Cos}\,\psi \tag{17}$$

where w_i and w_p are displacement of impactor and target plate displacement along global z direction at the impact point (x_c, y_c), respectively. Here ψ and ζ_i are the angle of twist and oblique angle, respectively. The components of force at the impact point in global directions are given by

$$P_{ix} = 0, \quad P_{iy} = C_f\,\mathrm{Sin}\,\psi \;\text{ and }\; P_{iz} = C_f\,\mathrm{Cos}\,\psi \tag{18}$$

3 Results and discussion

The results obtained from the computer codes developed on the basis of present finite element modelling are validated with those in the open literature both in respect of impact and delamination model. In Figure 3, the time histories of contact force are validated for ten layered symmetrically laminated cross-ply ($[0°/90°/0°/90°/0°]_S$) composite plate under simply supported boundary condition as analysed by Sun and Chen [2] using finite element method, while Figure 4 presents variation of natural frequencies of composite cantilever beam with relative position of the delamination as computed by Krawczuk et al. [12]. Present FEM employed eight noded isoparametric plate bending element with optimal time step of 1.0 μ-sec.

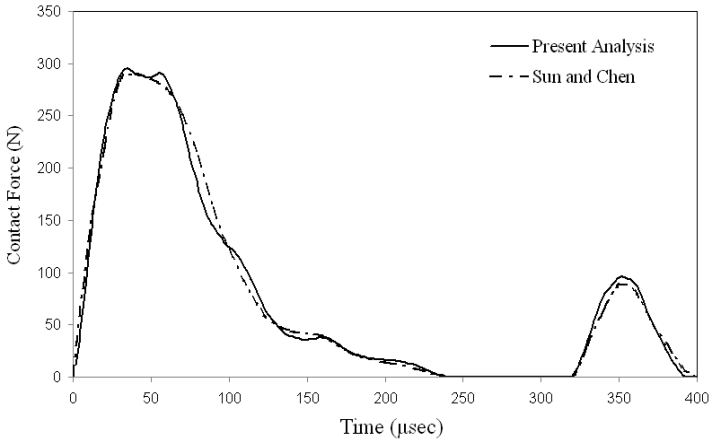

Figure 3: Time history of contact force for centrally impacted cross-ply ([0°/90°/0°/90°/0°]s) composite plate under simply supported condition with laminate dimension of 20 cm x 20 cm x 0.269 cm, mass density of impactor=7.96 x 10^{-5} N-sec^2/cm^4, time step=1.0 μ-sec, E_1=120 GPa, E_2=7.9 GPa, Ei=210 GPa, $G_{12}=G_{23}=G_{13}$=5.5 GPa, ρ=1580 kg/m^3, $\nu_i=\nu_{12}$=0.3, VOI=3 m/s [2]

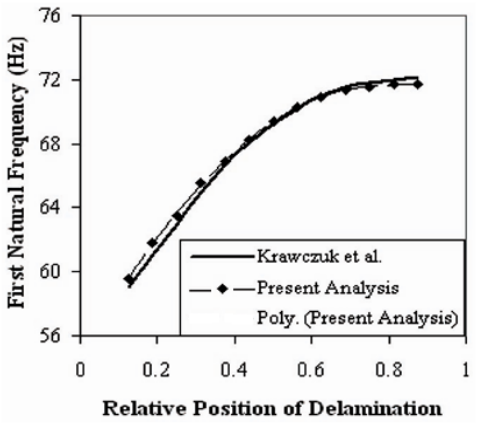

Figure 4: Relative position of delamination on first natural frequency of composite cantilever beam [12]

3.1 Transient response

Parametric studies are conducted for eight-layered mid-plane delaminated graphite-epoxy torsion stiff composite pretwisted conical shells subjected to low velocity oblique impact at the centre. The effect of twist angle on contact force histories for torsion stiff composite conical shell panel is furnished in Figure 5 wherein mid-plane delamination is considered with relative position of its centre line being 0.25 from the fixed end. Transient response is obtained for untwisted (Ψ=0°) and twisted (Ψ=45°) mid-plane delaminated torsion stiff composite conical shells. The maximum contact force which indicates the highest load withstood by the composite shell panel under low velocity oblique impact increases impact energy up to a threshold value and then to level off, thus stipulating the load carrying capability of the torsion stiff laminate.

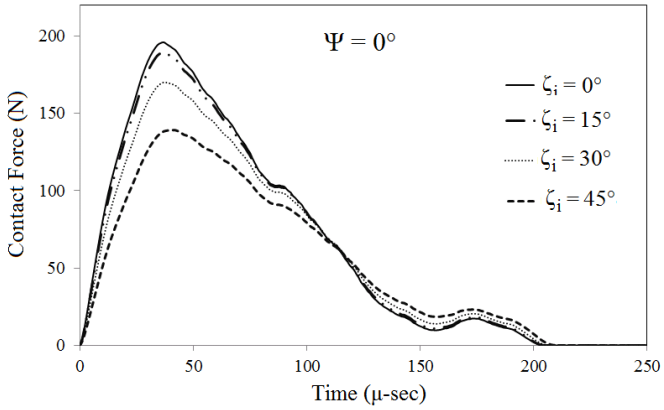

(a)

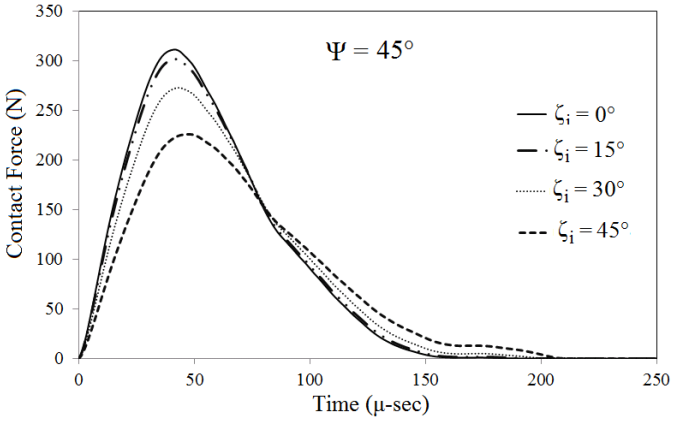

(b)

Figure 5: History of contact force with time for (a) untwisted and (b) twisted mid-plane delaminated graphite-epoxy torsion stiff [(45°/-45°/-45°/45°)s] composite pretwisted conical shells subjected to low velocity oblique impact, considering Δt=1.0 μ-sec, E_1=120 GPa, E_2=7.9 GPa, E_i=210 GPa, $G_{12}=G_{23}=G_{13}$=5.5 GPa, ρ=1580 kg/m^3, $\nu_i=\nu_{12}$=0.3, VOI=3 m/s, h=0.005 m, n=8, L/s=0.7, θ_o=45°, θ_v =20°.

The contact duration is found to be lower for twisted delaminated torsion stiff composite conical shell panels compared to untwisted one and it is found to increase with rise of oblique impact angle. In general, the peak value of contact force is found to increase with the rise of twist angle and maximum contact force of untwisted case is always found lower than that of corresponding twisted cases. Hence, it can be inferred that twist angle has significant effect on stiffness of the torsion stiff composite conical shells which in turn results in variation of contact force histories with respect to time.

3.2 Target displacement

The history of target displacement is a function of impact energy parameter. The energy absorbed in impact event (contact load-unloading cycle) could be identified from its target displacement. In the present analyses, the target displacement is found to be influenced in the light of transient dynamic response of delaminated composite conical shells as furnished in Figure 6.

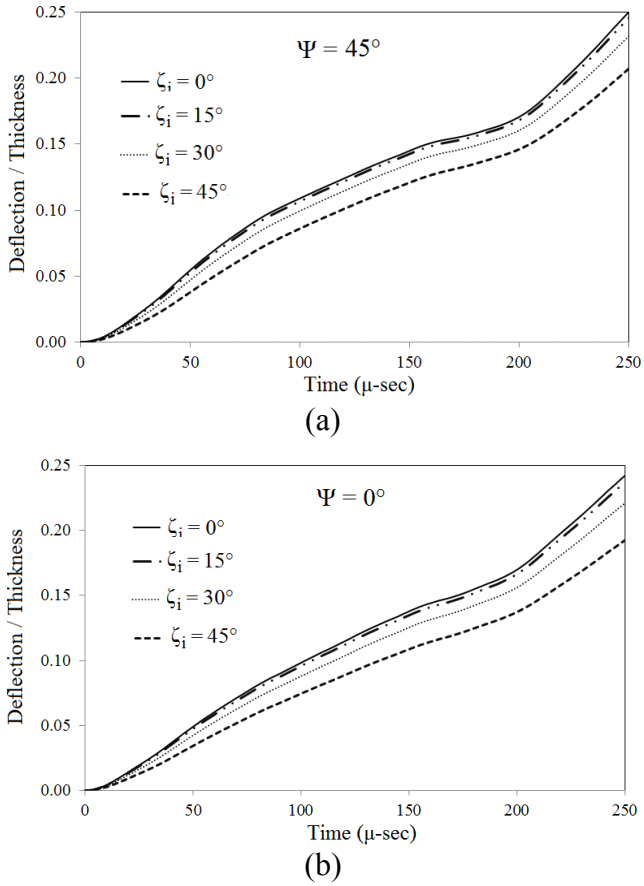

Figure 6: Effect of oblique angle on time histories of (a,b) deflection/thickness for mid-plane delaminated graphite-epoxy torsion stiff [(45°/-45°/-45°/45°)s] composite pretwisted conical shells considering Δt=1.0 μ-sec, E_1=120 GPa, E_2=7.9 GPa, E_i=210 GPa, $G_{12}=G_{23}=G_{13}$=5.5 GPa, ρ=1580 kg/m^3, $\nu_i=\nu_{12}$=0.3, VOI=3 m/s, h=0.005 m, n=8, L/s=0.7, θ_o=45°, θ_v =20°.

In general, the slope of deflection/thickness curve with respect to time is found to reduce with the increase of oblique impact angle irrespective of twist angle. Hence, during loading-unloading cycle, it is also observed that slope of deflection/thickness curve is inversely proportional to oblique impact angle. The slope of deflection/thickness for twisted torsion stiff shell panel is observed as slightly higher than that of untwisted one.

3.3 Displacement and velocity of impactor

The impactor's displacement and velocity are significantly found to be influenced in the light of transient dynamic response of delaminated composite conical shells as furnished in Figure 7 and Figure 8. For a particular initial velocity of the impactor, the slope of impactor's displacement is found to increase with rise of oblique impact angle irrespective of twist angle while the velocity of impactor is observed to reduce with time for both untwisted and twisted cases.

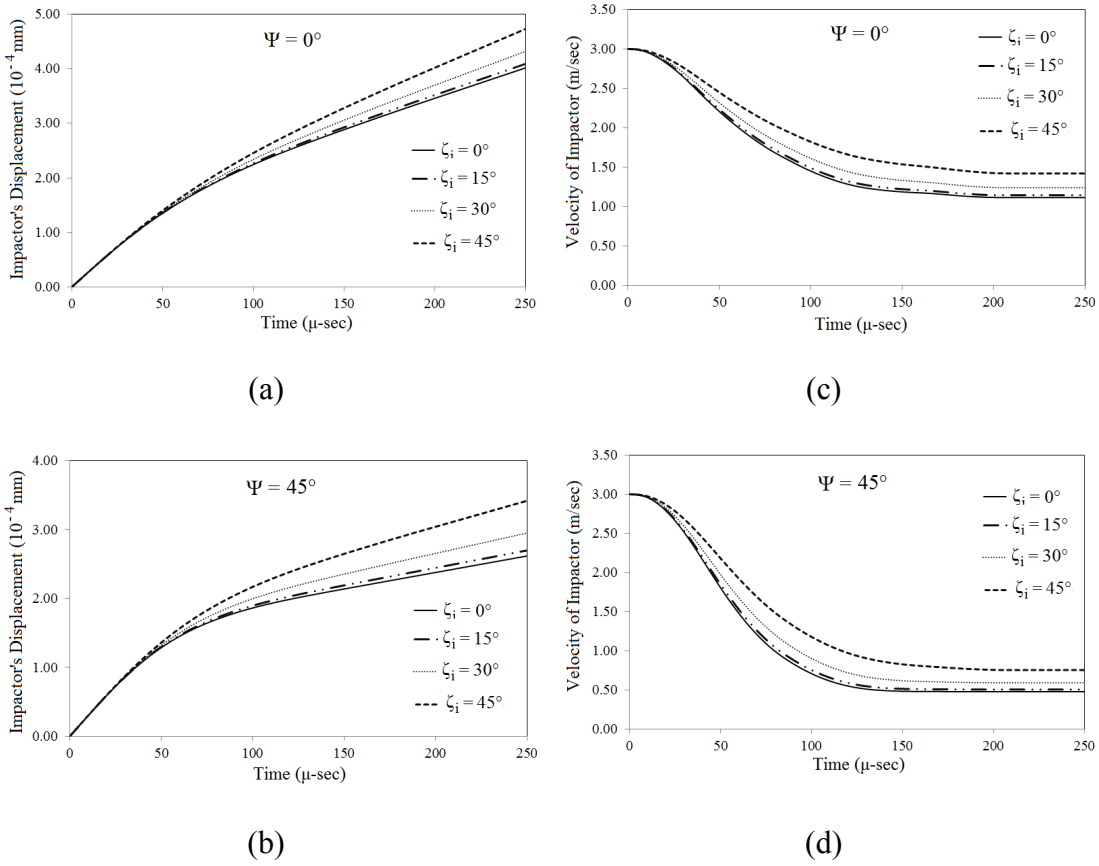

Figure 7: Effect of oblique angle on time histories of (a,b) Impactor's displacement (10^{-4} mm) and (c,d) Velocity of impactor (m/sec) for mid-plane delaminated graphite-epoxy torsion stiff [(45°/-45°/-45°/45°)s] composite pretwisted conical shells considering Δt=1.0 μ-sec, E_1=120 GPa, E_2=7.9 GPa, E_i=210 GPa, $G_{12}=G_{23}=G_{13}$=5.5 GPa, ρ=1580 kg/m^3, $\nu_i=\nu_{12}$=0.3, VOI=3 m/s, h=0.005 m, n=8, L/s=0.7, θ_o=45°, θ_v =20°.

4 Conclusions

The computer codes based on the present formulation is validated with the results published in open literature and hence, this can be applied to analyse the dynamic analysis for laminate configuration. In general, the peak value of contact force is found to increase with increase of angle of twist. The peak value of contact force of delaminated torsion stiff composite conical shell is found to reduce with increase oblique impact angle. The slope of deflection/thickness curves are found to decrease with the rise of oblique impact angle while the slope of impactor's displacement curve is observed to increase with increase of oblique impact angle irrespective of twist angle.

References

[1] M. S. Qatu and A. W. Leissa, "Vibration studies for laminated composite twisted cantilever plates", Int. J. Mechanical Sciences, 33(11), 927–940, 1991.

[2] C. T. Sun and J. K. Chen, On the impact of initially stressed composite laminates, Composite Materials, 19 (1985) 490–504.

[3] A. Karmakar A. and K. Kishimoto, "Transient dynamic response of delaminated composite rotating shallow shells subjected to impact", Shock and Vibration, 13, 619–628, 2006.

[4] P. K. Parhi, S. K. Bhattacharyya and P. K. Sinha, "Failure analysis of multiple delaminated due to bending and impact". Bull. Mater. Sci., 24(2), 143–149, 2001.

[5] C. K. Gim, "Plate Finite element modelling of laminated plates", Composite Structures, 52, 157-168, 1994.

[6] K. J. Bathe, "Finite Element Procedures in Engineering Analysis", New Delhi: PHI; 1990

[7] A. W. Leissa, J. K. Lee and A. J. Wang, "Vibrations of twisted rotating blades", J. Vibration, Acoustics, Stress, and Reliability in Design, Trans., ASME, 106(2), 251-257, 1984.

[8] A. Karmakar and P. K. Sinha, "Failure analysis of laminated composite pretwisted rotating plates", J. Reinforced Plastics and Composites, 20(14-15), 1326-1357, 2001.

[9] S. Sreenivasamurthy and V. Ramamurti, "Coriolis effect on the vibration of flat rotating low aspect ratio cantilever plates", J. Strain Analysis, 16(2), 97-106, 1981.

[10] S. H. Yang and C. T. Sun, "Indentation law for composite laminates", Composite Materials: Testing and Design, ASTM STP, 787, 425–446, 1982.

[11] A. Karmakar A. and P. K. Sinha, "Finite element transient dynamic analysis of laminated composite pretwisted rotating plates subjected to impact", Int. J. of Crashworthiness, 3(4), 379–391, 1998.

[12] M. Krawczuk, W. Ostachowicz and A. Zak, "Dynamics of cracked composite material structures", Computational Mechanics, 20, 79-83, 1997.